Desalination and Water Treatment
www.deswater.com
doi: 10.5004/dwt.2019.24182

158 (2019) 245–255
August

Comparison treatment of cyanide by chemical precipitation, Fenton and fluidized-bed Fenton process with suspended carrier coated iron oxide: parameter optimization and mechanism

Jiawei Tang[a], Xuelu Shi[a], Chao Sun[a], Honglei Zhuang[b], Ke Ning[c], Chunhui Zhang[a,*]

[a]*School of Chemical & Environmental Engineering, China University of Mining & Technology, Beijing 100083, China, Tel./Fax: +86 10 6233 9331; emails: ZCHcumtb@hotmail.com (C. Zhang), angpdh24tjw@hotmail.com (J. Tang), stealusxl@163.com (X. Shi), sunkconfession@163.com (C. Sun)*
[b]*Xizang Sinorichen Environmental Protection Co., Ltd., Naidong district, Tibet Autonomous Region, 856100, China, email: 973785442@qq.com*
[c]*Environmental Protection Research Institute of Light Industry, Beijing 100012, China, email: nkmyshelf@qq.com*

Received 25 November 2018; Accepted 27 March 2019

ABSTRACT

A fluidized-bed Fenton reactor was employed and compared with chemical precipitation and homogeneous Fenton process for the treatment of cyanide-containing wastewater using polypropylene light materials coated with iron oxides as suspended carriers. Under the optimal operating conditions that the initial pH of 3.0, H_2O_2 concentration of 6 mL/L, Fe^{2+} dosage of 0.24 g/L, carrier dosage volume of 40%, and aeration flow rate of 0.22 m^3/h with 80 min of reaction time, chemical oxygen demand and cyanide were removed by 87.8% and 83.6%, which facilitate a high removal rate and low level of Ferrous ion consumption. The suspended carriers coated with iron oxides used in this study display outstanding stability, suggesting that the proposed process can be an effective way for treatment of cyanide-containing wastewater.

Keywords: Cyanide-containing wastewater; Fluidized-bed Fenton process; Iron oxide; Suspended carrier

1. Introduction

Driven by increasing demand, chemical fiber industry has rapidly progressed in China that lead to large amounts of wastewater containing cyanide and organic contaminants were inevitably produced in the chemical fiber production process during the past few decades [1,2]. Cyanide is reported acutely toxic to living organisms, exposure to even small amounts of cyanide can lead to inactivation of the enzyme cytochrome oxidase, resulting in inhibition of cellular respiration, manifesting as tumors, nerve damage, or even death [3]. It has been proven that cyanide enters the environment mainly through wastewaters originating from industrial activities such as metal plating, steel manufacturing, production of chemical fertilizers, organic chemicals, coal coking, oil refining, mining, electronics manufacturing and photography industries [4,5]. Generally, synergistic anaerobic-aerobic methods, alkaline chlorination processes, ion exchange methods, and activated carbon biological treatments are used for the treatment of cyanide-containing wastewater. The most common processing methods and their characteristics are summarized in the following Table 1 [6].

Among these technologies, however, due to the inhibitory effect of cyanide on micro-organisms, and the fact that cyanide tends to strongly bind with metals, thereby deactivating essential metalloenzymes, as a result it is ineffective to degrade cyanide by biological treatment process [7–9]. Besides, ozone oxidation, extraction, and ion exchange possess good remove effect but need to pay a huge cost.

* Corresponding author.

Table 1
Summary of treatment methods of cyanide containing wastewater

Methods	Advantages	Limitations	Applicable concentration	Cost
Alkaline chlorination process	Less investment and effective treatment	Complex process and serious equipment corrosion	Higher	Higher
Chemical complex precipitation	Simple operation	Large amount of precipitation and waste residue	Higher	Low
Ozone oxidation	Simple operation without adding other pollutants	High power consumption	Lower	High
Activated carbon	Simple process with low cost	High cost of activated carbon and regeneration frequency	Low	Lower
Electrolysis	Less ground demand	High energy consumption	High	High
Extraction	No waste liquid production; recoverable metal	Complex operation with high cost	High	Higher
Ion exchange	Good purification effect, recyclable metal	Resin is expensive and complicated to operate	Low	High
Wet air oxidation	Complete oxidation without secondary pollution	Large one-time investment and strict equipment requirements	High	High
Biodegradation	Strong applicability and better water quality	Harsh operating conditions and large investment	Low	Commonly

advanced oxidation processes (AOPs) post biological treatment is preferred as the potential technologies for treating refractory compounds in wastewater [10]. Although ozone and wet air oxidation methods reach high levels of cyanide removal, the cost of investment is too large that restricting application. Fenton process (using Fenton's reagent), as a matured AOP technology, has been proven very effective in removing various organic contaminants with simple operation [11]. Fenton's reagent is a mixture of hydrogen peroxide and Fe^{2+} applied at acidic pH to generate hydroxyl radical ($^{\bullet}OH$) [12]. Wei et al. [1] have successfully applied Fenton process as the pretreatment of wastewater from dry-spun acrylic fiber manufacturing and achieved efficient results. However, the Fenton process is expensive to operate because of the large amount of reagent consumed, including Ferrous ion, hydrogen peroxide, and acid solution [13]. Another major disadvantage of Fenton's process is the production of large volumes of $Fe(OH)_3$ sludge upon pH neutralization post treatment. Even after dewatering, this bulky sludge typically contains up to 80% water [14]. To address this problem, the volume of $Fe(OH)_3$ sludge can be reduced using iron oxides in a fluidized-bed reactor as catalyst for oxidizing organic contaminants, which can acquire a goal of turning waste into treasure [15]. The $Fe(OH)_3$ product from the Fenton process can be crystallized and grow on the surface of some carriers in fluidized-bed Fenton systems, which reduces the precipitation of $Fe(OH)_3$ [16]. Early study has been reported and applied a fluid-bed Fenton system using three different carrier substrates (quartz sand, brick particles, and granular activated carbon) for the treatment of recalcitrant organic silicone wastewater and acquired satisfactory removal efficiencies of chemical oxygen demand (COD) and TOC [17].

Previous studies on carriers have focused on the quartz and activated carbon, however, the operating cost of this is considerably higher due to the high density of these carriers. Herein the study utilized polypropylene light materials as carriers in the fluidized-bed Fenton process to obtain a highly efficient system with practical applicability for advanced treatment of cyanide-containing wastewater from a chemical plant. Multi-group experiments were performed and compared to establish the optimal conditions and respective issues relevant to this work. Included in this research, were the questions of whether iron-oxide can be coated on the surface of polypropylene light materials stably as expected, and whether higher removal efficiencies can be achieved comparing chemical precipitation, and Fenton oxidation by the iron-oxide-coated suspended carriers in the heterogeneous catalytic treatment process.

2. Materials and methods

2.1. Wastewater collection

The cyanide-containing wastewater used in this study was collected from the effluents after pretreatment (sedimentation tank) of wastewater treatment plant (WWTP, A/O technology) from Jilin Qifeng Chemical Fiber Co. Ltd., (Jilin Province, China). The wastewater samples were collected three times within 24 h and were well mixed with equal volume. The above samples were stored at 4°C under a refrigerator until sample pretreatment. The main wastewater characteristics are presented in Table 2.

2.2. Reagents and materials

The analytical reagents of NaOH (5.0 M) and H_2SO_4 (3.0 M) were purchased from Beijing Chemical Reagent Co., Ltd., China. The ferrous sulfate ($FeSO_4{\cdot}7H_2O$) and hydrogen peroxide (H_2O_2, 30%) were purchased from Beijing Lanyi Chemical Co., Ltd., China. All chemicals were at least

Table 2
Characteristics of cyanide-containing wastewater treated after pretreatment process

Parameter	Mean value
pH	5.8
COD_{Cr}, mg/L	605
BOD_5, mg/L	9–13
NH_3–N, mg/L	63
TN, mg/L	98
Cyanide, mg/L	28

of analytical grade and were used as received without any further purification treatments.

Two kinds of polypropylene light materials, which were marked as YL-1 and YL-2 (Fig. 1) with different volume and specific surface area, were used as suspended carriers in the Fenton fluidized-bed system. The suspended carriers were purchased from Xizang Sinorichen Environmental Protection Co. Ltd. (China). The main characteristics of suspended carriers were presented in Table 3.

2.3. Experimental process design

2.3.1. Chemical precipitation procedure

CN^- can combine with various metal ions to form stable complexes, but most of the complexes are innocuous and harmless. Therefore, Fe^{2+} is often used to generate $[Fe(CN)_6]^{4-}$ precipitate for the removal of CN^-. $FeSO_4{\cdot}7H_2O$ is commonly used as precipitant because of its inexpensiveness and applicability. The precipitation process can be described by the following reactions:

$$6CN^- + Fe^{2+} \rightarrow \left[Fe(CN)_6\right]^{4-} \quad (1)$$

$$Fe(CN)_6^{4-} + 2Fe^{2+} \rightarrow Fe_2\left[Fe(CN)_6\right]\downarrow \quad (2)$$

The total reaction formula is:

$$6CN^- + 3FeSO_4 \cdot 7H_2O \rightarrow Fe_2\left[Fe(CN)_6\right]\downarrow + 3SO_4^{2-} + 2H_2O \quad (3)$$

It is deduced that the CN^- can form an iron complex with a coordination number of 6 with both Fe^{2+} and Fe^{3+}. Based on the chemical equation above, when Fe^{2+} and CN^- react to produce iron-blue ($Fe_4[Fe(CN)_6]_3$, $K_{sp} = 1 \times 10^{-42}$), the mole ratio between Fe^{2+} and CN^- (n_{Fe2+}/n_{CN^-}) is 18:7. According to the cyanide concentration in the wastewater (28 mg/L), the theoretical dosage of $FeSO_4{\cdot}7H_2O$ is 0.116 g/L after calculation. In this experiment, different pH levels, reaction times, and dosages of Ferrous sulfate were investigated.

2.3.2. Traditional Fenton procedure

Fenton oxidation experiments were conducted in 500 mL batch reactors at 25°C with mechanical stirring for continuous mixing of the reaction system. The pH was adjusted by 3.0 M H_2SO_4 solution and 5.0 M NaOH solution. In a typical experiment, a weighed amount of $FeSO_4{\cdot}7H_2O$ was dissolved in 300 mL of wastewater sample with stirring (120 rpm). Fenton oxidation was then initiated by the addition of H_2O_2 solution (30%, w/w). On the basis of COD concentration (605 mg/L), theoretical dosage of H_2O_2 was calculated to 3.86 mL/L. Then the actual amount of 4 mL/L was weighed to reduce the personality error. Previous

Table 3
Main characteristics of suspended carriers

Parameter	YL-1 carrier	YL-2 carrier
Specifications (Φ × H, mm)	10 × 10	25 × 9
Specific gravity (g/cm^3)	0.9613	0.9627
Accumulation amount (1 L)	500	110
Effective surface area	850 m^2/m^3	532 m^2/m^3
Void volume (%)	>85	>90

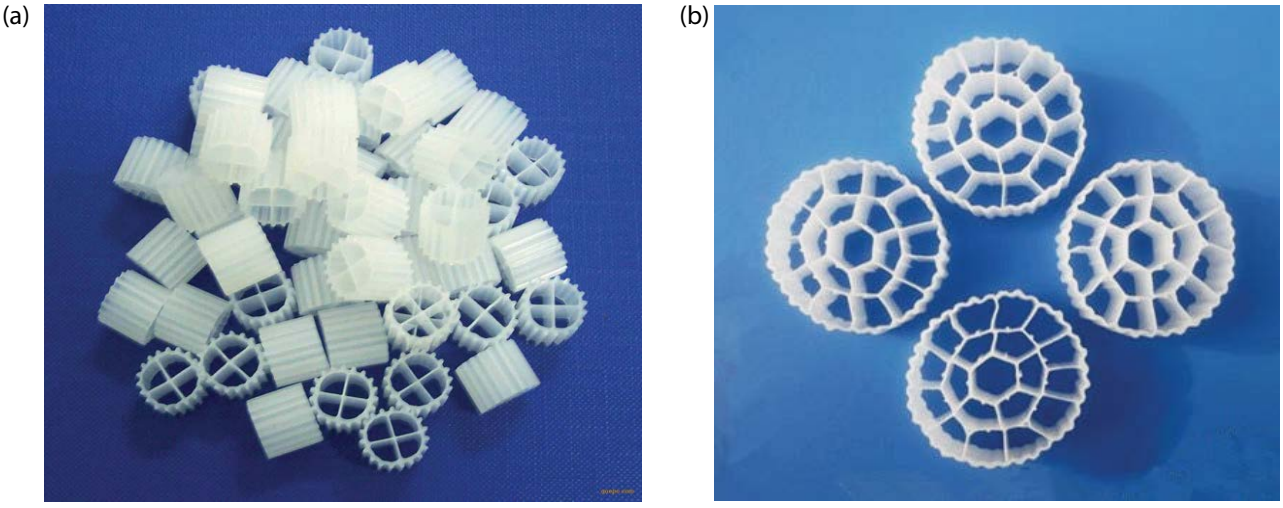

Fig. 1. Physical images of YL-1 (a) and YL-2 (b) suspended carriers.

studies had proved that traditional Fenton process could play maximum efficiency in an acid solution (pH = 3) [18,19]. Hence, different Fe^{2+} (0.15, 0.3, 0.45, and 0.6 g/L) and H_2O_2 (2, 4, 6, and 8 mL/L) concentration were tested and analyzed to obtain optimum parameters under the conditions of pH 3, and room temperature (25°C).

2.4. Preparation and characterization of iron oxide coated suspended carrier

The suspended carriers were soaked in H_2SO_4 solution (pH = 1.0) for 24 h first, then washed with deionized water until the rinse effluent pH was 7.0 before air drying (48 h at room temperature). After that, the suspended carriers were put into the fluidized-bed Fenton reactor, and leached by solutions consisted of hydrogen peroxide (H_2O_2, 10 mmol/L, 5 L) and ferrous sulfate ($FeSO_4{\cdot}7H_2O$, 10 mmol/L, 5 L) with flow velocity of 10 mL/min for 15 d. Upper influent and lower effluent of solution were used in the leaching process with a recycling way. Finally, a layer of dense brown precipitate was attached on the surface of carriers, which indicated the suspended carriers coated with iron oxide were prepared well. Well-prepared suspended carriers were put into the acidic solution to prepare for future use. More details on the preparation of the catalytic carrier in the early report [20].

Fig. 2 shows the physical images of suspended carriers after coating. As displayed in the figure, the surface of the suspended carrier changes from white to brown, which coated with a dense layer of iron oxide precipitation. More characterizations of suspended carriers were validated by examining the surface of carriers before and after coating by SEM and XRD analysis in follow up.

2.5. Fluidized-bed reactor setup

The experimental reactor operated in this study was made of plexiglass column with a diameter of 100 mm and a height of 600 mm which is as shown in Fig. 3. The effective volume of the reactor is about 3 L. The wastewater was introduced into the bottom of the reactor via peristaltic pump, and the treated effluent was discharged at the top of the reactor. An air compressor (China) was used to produce air supply for the reactor. A 50 mm cylindrical micropore titanium plate placed at the bottom of the reactor was used to generate macro-bubbles (mean bubble size of about 1 mm). The aeration rate was set at 0.2 m^3/h in operation preliminarily. The suspended carriers were packed above on the layer of glass drops. At the beginning of the experiment, water sample was pumped into the reactor. The initial pH was adjusted to reactor operating at a pH of 3.0. Then, the Fenton reagent was pumped into the reactor from the bottom side using a micro-peristaltic pump with a flow rate of 3 mL/h. A stable pH of 3.0 was maintained in the reactor by adding H_2SO_4 or NaOH during the process operation. Besides, it is crucial for catalyst to keep stable catalytic activity and reusability in catalyzed reactions. Either the poor stability or severe deactivation will fail in its practical industrial application. So the recycling performance of these catalytic carriers was evaluated after four recycling of utilization under the optimal experimental parameters.

2.6. Analytical methods

The wastewater was analyzed for various parameters according to standard methods of China [20]. COD was determined using potassium dichromate titration method (GB 11914-89, China), TN was determined by alkaline potassium persulfate oxidation-UV spectrophotometric method (GB 11894-89, China), cyanide was performed using UV spectrophotometry (HJ 484-2009, China), and the pH value was measured by a Shanghai Leici PHS-3D brand pH-meter. TOC was determined using a TOC analyzer (TOC-V CPH Shimadzu, Japan). A MERLIN Compact scanning electron microscopy (SEM, German) was employed to characterize the morphological change of suspended carriers, and the composition of iron oxide was analyzed using XRD after drying the samples at 105°C for overnight. The total iron concentrations were determined using atomic absorption spectrometer (Shimadzu AA6300, Japan). The amount of iron loaded over the surface of carrier was measured by strong acid immersion dissolution method, which the carrier loaded with iron was immersed in hydrochloric acid (30%, w/w) to dissolve completely before the determination of iron concentration in solution, more details have been summarized in our

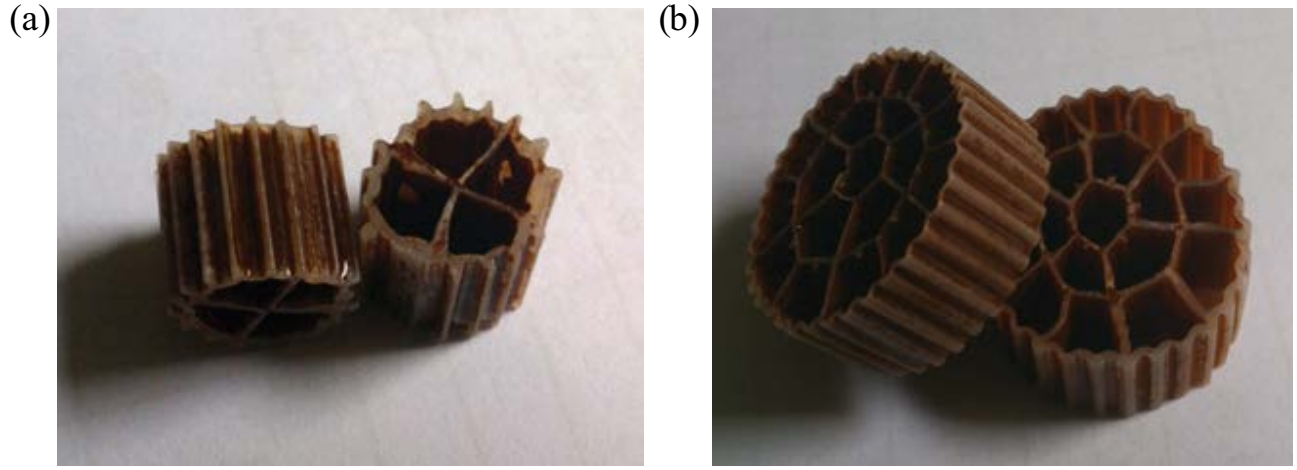

Fig. 2. Surface images of YL-1 (a) and YL-2 (b) suspended carriers after coating.

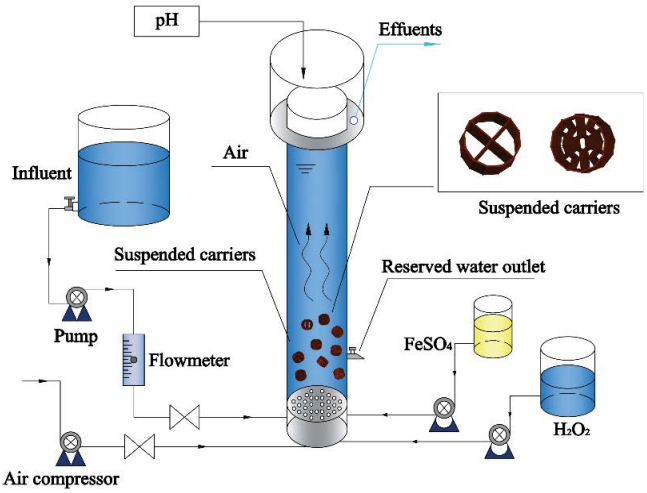

Fig. 3. Schematic diagram of fluidized-bed Fenton reactor.

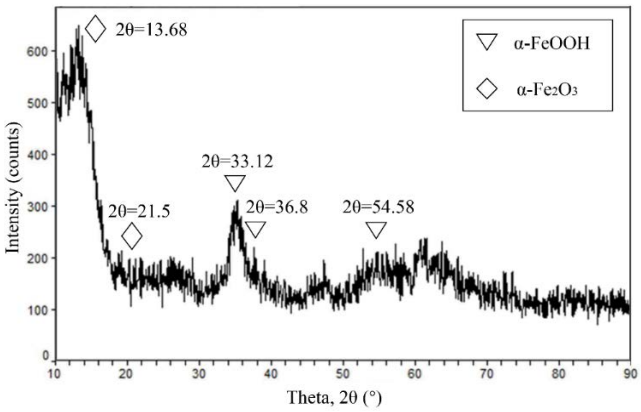

Fig. 5. Energy dispersive X-ray spectroscopy of Fe-oxides.

previous study [20]. The percentage of pollutant removal was calculated by the following expression:

$$\%\text{Removal} = \frac{\left(C_0 - C_t\right)}{C_0} \times 100 \quad (4)$$

where C_0 and C_t are the pollutant concentration (mg/L) at the initial and t time of reaction.

3. Results and discussion

3.1. Characterization of the iron oxide coated suspended carrier

The SEM analysis was carried out on the suspended carrier coated with iron oxides. The SEM images of Figs. 4a–c were captured by In-Lens detector. In the same test conditions, the SEM images of Figs. 4d–f were captured by ESB detector. As presented, after coating with iron oxides, a uniform film was observed on the surface of suspended carriers. Large pores existed among iron oxides, which suggested that iron oxide film on carrier surface was not composed of single layer but multilayer.

In order to determine the presence of iron oxide components on the surface of coated carriers, the X-ray spectroscopy analysis was conducted, and the result reveals that the iron oxides were mainly composed of Fe, O, and S elements (Fig. 5). The Fe content was as high as 45.34%, and 47.17% in YL-1 and YL-2 carrier, respectively. In these experiments, it could be deduced that the iron oxides on the carriers were mainly amorphous FeOOH, Fe_2O_3 and Fe $(OH)_3$ as the reaction occurred in the presence of hydrogen peroxide at low pH [21]. Besides, the densities of suspended carriers

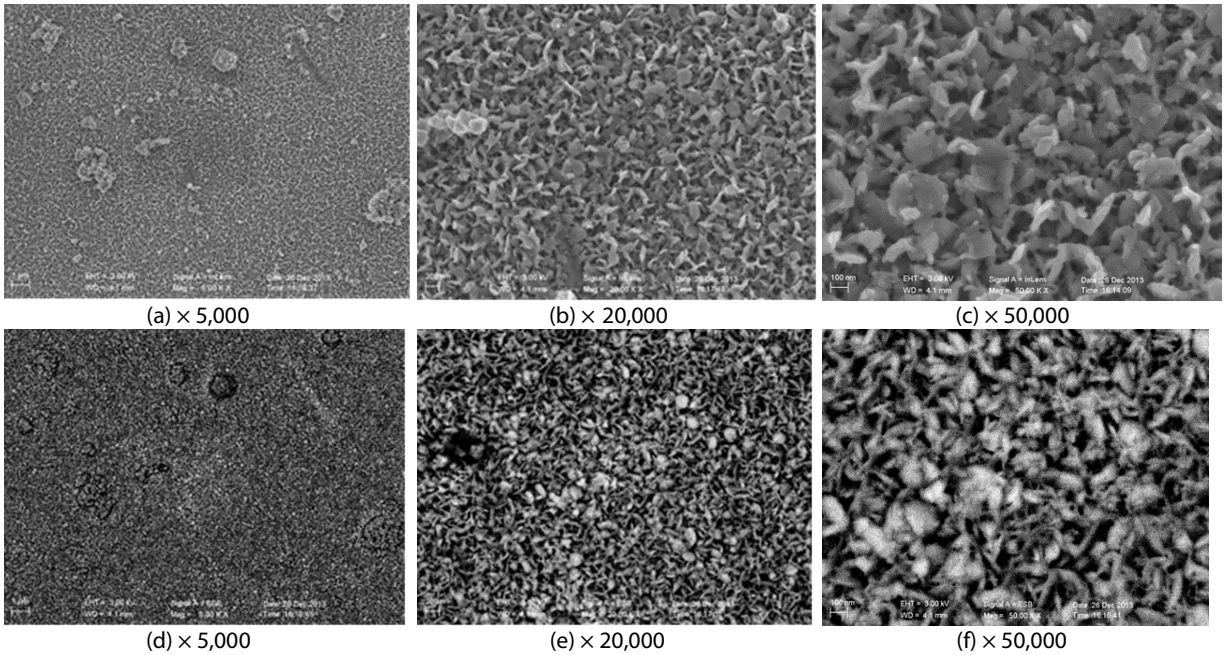

Fig. 4. SEM images of suspended carrier coated with iron oxides ((a–c) were detected by InLens detector and (d–f) were detected by ESB detector).

were determined by specific gravity method. According to the measurement results, the density of the YL-1 and YL-2 carrier was 1.0125 and 1.0218 g/cm^3 after coating, which increased by 0.0512 and 0.0591 g/cm^3, respectively. Under mild aeration, the coated carriers can be in fluidization in the fluidized-bed Fenton process. Compared with other types of carriers [21], the light density carriers used in this study need less aeration in running that lead to an energy-saving in the fluidized-bed Fenton reactor as a result.

The content of coated iron oxides indicates the catalyst content of suspended carrier. And the adhesion strength determines the stability of the catalyst. The loads and intensities of two suspended carriers are presented in Table 4.

It can be concluded from Table 4 that a large amount of iron oxides were loaded on two kinds of carriers, especially YL-2 carrier shows strong loading capacity (91.7 mg per carrier) in cyclic immersion method due to its special structure. Compared with the loading ability of quartz sands according to the former research [22], the suspended carriers used in our study can load more iron oxides. Moreover, the dissolvability of YL-1 carrier and YL-2 carrier were 3.82% and 3.79% in acidic solution (pH of 2), 10.24% and 10.71% in alkaline solution (pH = 12), respectively, that exhibit better performance of adhesive strength and adaptability.

3.2. Parameters optimization of chemical precipitation process

On the basis of calculation of Eq. (3), various quantities of Fe^{2+} (1–3 times the stoichiometric amount) were added to the reactor under the same conditions (stirring for 40 min, pH 6) to verify the optimum operating parameters in the actual process. The results obtained are shown in Fig. 6.

As indicated in Fig. 6, an increase in ferrous ion dosage corresponds to an increase in the removal rate of cyanide. Maximum removal efficiency of approximately 75% occurred when the ratio of actual dosage to the predicted value was 1.9 or more. At the beginning of the reaction, the $Fe_2[Fe(CN)_6]$ precipitate was generated from the reaction between CN^- and Fe^{2+}. Later, it was further converted into $Fe_4[Fe(CN)_6]_3$ following contact with air. On the contrary, the addition of ferrous sulfate would lead to coagulation and sedimentation process. As a result, the generated flocs sank to the bottom by wrapping colloids and suspended substances to achieve

Table 4
Loads and intensities of two suspended carriers

Parameter	YL-1 carrier	YL-2 carrier
Load iron content (mg/each carrier)	30.46	91.72
Dissolvability in acidic solution (mg/each carrier)	1.16	3.48
Adhesive strength in acidic solution (%)	3.82	3.79
Dissolvability in alkaline solution (mg/each carrier)	3.12	9.82
Adhesive strength in alkaline solution (%)	10.24	10.71

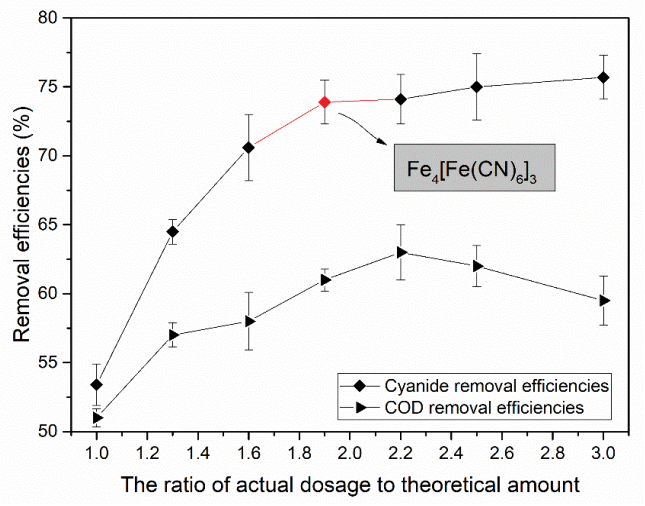

Fig. 6. Effect of $FeSO_4{\cdot}7H_2O$ dosage on cyanide removal (stirring time: 40 min, pH 6).

the goal of reducing COD in wastewater. However, excessive ferrous dosage would lead to an increase of COD due to the reducibility of ferrous ions. Therefore, batch experiments were conducted and simulated to further study the effect of pH and stirring time under optimum conditions (0.22 g/L of Fe^{2+} dosage for initial cyanide concentration of 28 mg/L). The results (Fig. 7) show that the cyanide removal was optimized when the pH and stirring time were 5.0–6.5, and 33–40 min, respectively. An increase in stirring time could accelerate the precipitation reaction due to more contact with the air. When the pH exceeded 6.5, the cyanide removal effect dropped sharply, which could be expounded in the following chemical formula:

$$Fe_4\left[Fe(CN)_6\right]_3 + 12OH^- \rightarrow 4Fe(OH)_3\downarrow + 3\left[Fe(CN)_6\right]^{4-} \quad (5)$$

The decline in cyanide removal at higher pH could be ascribed to the increase of OH^-, which caused the

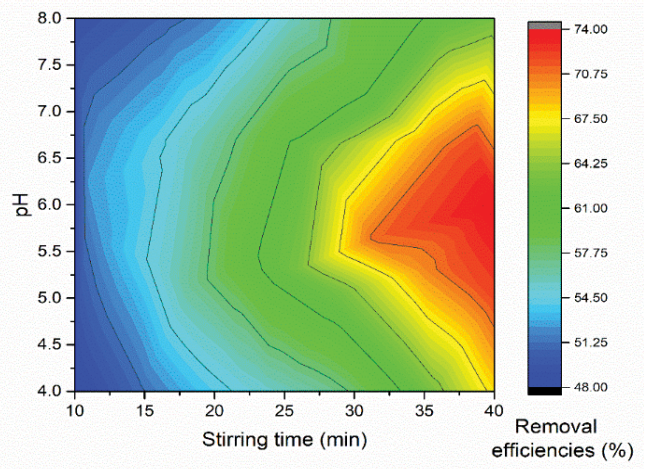

Fig. 7. Effect of pH and stirring time on cyanide removal (Fe^{2+} dosage: 0.22 g/L, initial cyanide concentration of 28 mg/L).

refractory precipitation to be decomposed into the soluble $[Fe(CN)_6]^{4-}$ resulting in a rise of cyanide concentration. Thus, Fe^{2+} dosage of 0.22 g/L and stirring time of 40 min at pH 6 were the optimum conditions in the chemical precipitation operation causing the cyanide concentration to be lowered to 7.28 mg/L.

3.3. Parameters optimization of Fenton process

The solution pH was adjusted to 3.0 by adding H_2SO_4, and the ferrous ($FeSO_4{\cdot}7H_2O$) solution was added after the pH reading was stabilized. The reaction began when the H_2O_2 solution was added. According to the results of chemical precipitation test and the theoretical dosage of H_2O_2 calculated by COD content, different dosage of Fe^{2+} (0.15–0.6 g/L) and H_2O_2 (2–8 mL/L) was investigated and stimulated in another batch experiments. The cyanide and COD removal effect is shown in Fig. 8.

From the above simulation diagrams, the Fe^{2+} and H_2O_2 dosage played an important role on the COD (Fig. 8a) and cyanide (Fig. 8b) removal efficiencies. Comparing with the chemical precipitation, the Fenton process is superior in the elimination of cyanide and COD as their removal rates increased by 12% and 23%, respectively, which attributed to the Fe^{2+} catalyzing H_2O_2 to generate $^{\bullet}OH$ radicals. Cyanide removal increased as the H_2O_2 concentration increased from 2 to 6 mL/L, and then changed insignificantly when the H_2O_2 concentration was further increased to 8 mL/L. The reaction mechanism of the Fenton process is described by the following formula:

$$Fe^{2+} + H_2O_2 \rightarrow Fe^{3+} + {}^{\bullet}OH + OH^- \quad (6)$$

When the content of Fe^{2+} in the solution is low, the decomposition rate of H_2O_2 slows correspondingly, resulting in less $^{\bullet}OH$ radical generation. Furthermore, it was deduced from the three-dimensional contour figure above, the optimal conditions for the Fenton process were pH 3, H_2O_2 concentration of 6 mL/L, and Fe^{2+} dosage of 0.48 g/L at room temperature (23°C ± 3°C).

3.4. Results and optimization of fluidized-bed Fenton process

The aeration flow rate, pH, carrier dosage volume, Fe^{2+}, and H_2O_2 dosage were the key factors for fluidized-bed procedure [23]. In order to systematically verify the practical application of the suspended carrier and the operation effect of the fluidized-bed Fenton system, batch tests were prepared and carried out. The following experiments were conducted to evaluate the cyanide removal efficiencies which included: (a) fluidized-bed Fenton without suspended carriers; (b) fluidized-bed Fenton with YL-1 carrier, without coating iron oxides, (c) fluidized-bed Fenton with YL-2 carrier, without coating iron oxides, (d) fluidized-bed Fenton with YL-1 carrier coating iron oxides, (e) fluidized-bed Fenton with YL-2 carrier coating iron oxides. The experiments were conducted at the following optimal conditions (Table 5).

The cyanide removal efficiencies of five experiments are presented in Fig. 9. It can be seen clearly that the distinction in different reaction systems was obvious. The process "b and c" have the worst effect, instead, process "a, d and e" have obtained good removal effect. As a catalyst, iron oxide is an important factor that can achieve more rapid degradation of organic compounds in Fenton process [24]. After 120 min of reaction time, the fluidized bed Fenton with suspended carriers without coating iron oxides and conventional Fenton process were able to degraded about 45%, and 60% of cyanide with 0.48 g/L of ferrous iron dosage, while process "d and e" achieved 83% of degradation ratio with half amount of ferrous iron. This comparison shows clearly that the cyanide removal efficiencies with suspended carriers coated with iron oxides were significantly higher than other Fenton processes, suggested that iron oxides coated on the suspended carriers had a good catalytic oxidation effect on the degradation of cyanide. Furthermore, the removal obtained from process "e" was higher than process "d" that could be attributed to the YL-2 carrier has larger specific surface area and more iron oxide that lead to a higher catalytic oxidation and degradation ability. Thus, the system of fluidized-bed Fenton with YL-2 carrier coating iron oxides and 80 min of reaction time were selected as the optimal system in the following experiments.

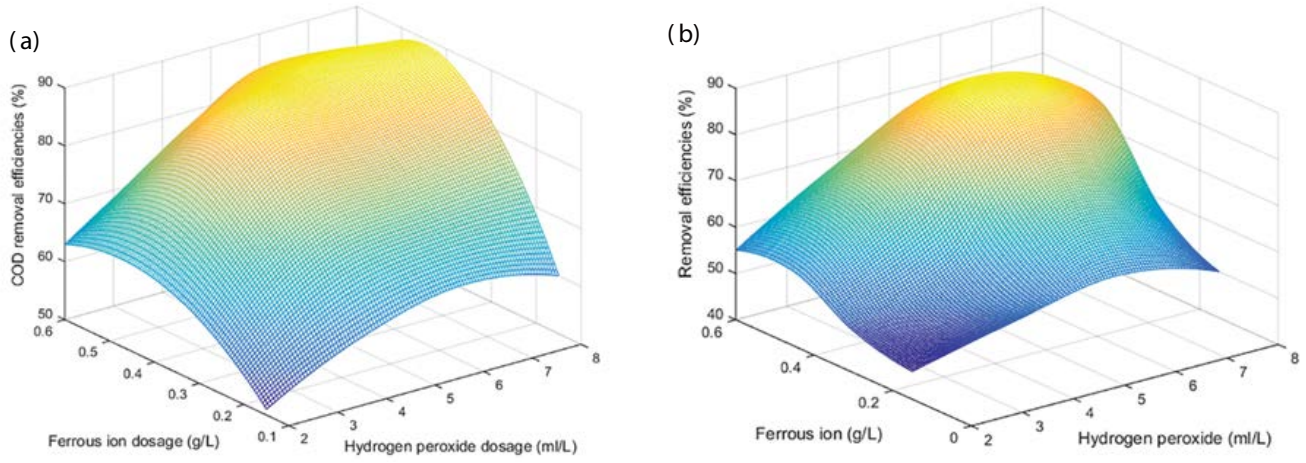

Fig. 8. Simulation study on removal efficiency of COD (a) and cyanide (b) by ferrous ion and hydrogen peroxide dosage (dosage of Fe^{2+}: 0.15–0.6 g/L, H_2O_2: 2–8 mL/L, pH of 3, initial COD and cyanide concentration was 605, 28 mg/L, respectively).

Table 5
Conditions for different systems

Process	No.	Reaction conditions				
		pH	H_2O_2 (mL/L)	Carrier volume	Fe^{2+} (g/L)	Aeration flow rate (m^3/h)
Fluidized-bed Fenton without suspended carriers	A	3	6	–	0.48	0.2
Fluidized-bed Fenton with YL-1 carrier, without coating iron oxides	B	3	6	40%	0.24	0.2
Fluidized-bed Fenton with YL-2 carrier, without coating iron oxides	C	3	6	40%	0.24	0.2
Fluidized-bed Fenton with YL-1 carrier coating iron oxides	D	3	6	40%	0.24	0.2
Fluidized-bed Fenton with YL-2 carrier coating iron oxides	E	3	6	40%	0.24	0.2

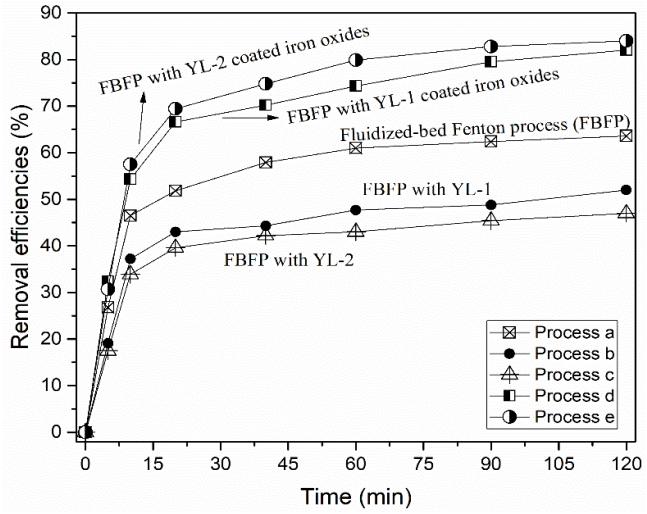

Fig. 9. Cyanide removal efficiencies in different systems.

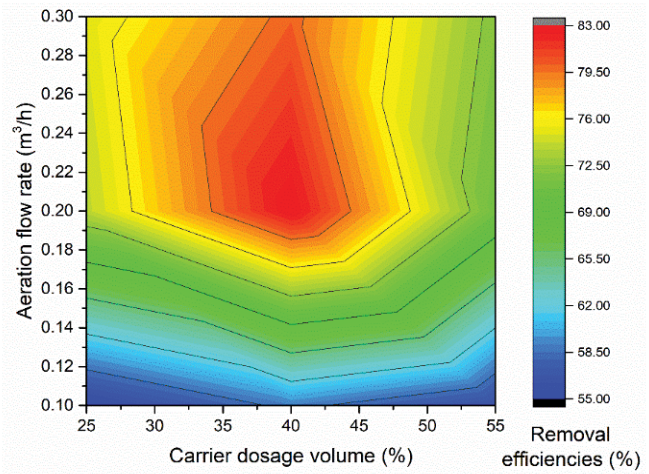

Fig. 10. Effect of different YL-2 carrier dosage volume and aeration flow rate on the removal of cyanide.

3.4.1. Effect of carrier dosage and aeration flow rate

In order to further verify the optimal values of these parameters, single-factor experiments were carried out by adjusting the solution pH to 3.0 under the initial H_2O_2 concentration of 6 mL/L, Fe^{2+} dosage of 0.24 g/L. Different aeration flow rate (0.1–0.3 m^3/h) and YL-2 carrier dosage volume (25%–55%) on cyanide removal efficiencies were added and investigated in this fluidized-bed Fenton reactor. Fig. 10 shows that during the early stage of the reaction, the cyanide removal efficiencies increased considerably with the addition rate of suspended carriers since the fact that an increase of carrier dosage volume led to the coated iron oxides on the carriers offered excess of Fe^{2+}, and shifted the chemical equilibrium that resulted in an accelerated reaction and greater generation of •OH radicals [25]. Whereas the carrier dosage volume exceeded 45%, the cyanide degradation increased slightly that might be ascribed to the excessive carrier volume had led to some secondary reactions to reduce the main reaction rate as well as the cyanide removal efficiencies [24,26]. Thus, removal of 83.6% was observed at the optimum parameters of carrier dosage volume 40% ± 3% and aeration flow rate 0.22 ± 0.04 m^3/h with 80 min of reaction time.

3.4.2. Effect of Fe^{2+} dosage and H_2O_2 concentration

Fig. 11 shows the effect of Fe^{2+} and H_2O_2 concentration on the removal efficiency of cyanide-containing wastewater. As expected, the cyanide removal efficiencies in the fluidized-bed Fenton process increased as the Fe^{2+} concentration was increased. Similarly, the degradation of cyanide increased as the H_2O_2 concentration increased from 4 mL/L to 8 mL/L, and then changed insignificantly when the H_2O_2 concentration was further increased to 10 mL/L. Generally, the H_2O_2 concentration is directly related to the amount of hydroxyl radicals produced in the Fenton process. The degradation rate of cyanide and organic compounds usually rise with increasing concentration of H_2O_2 until a critical value is reached. However, when the concentration is higher than the critical value, the degradation rate usually decreases with higher H_2O_2 concentration for the H_2O_2 acting then as a radical scavenger effectively changing the more reactive •OH

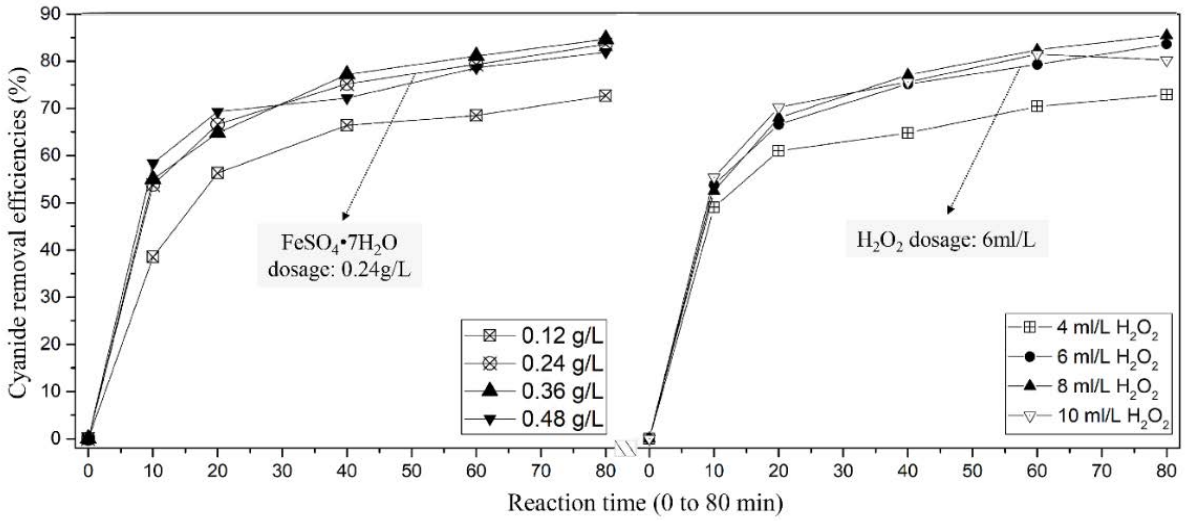

Fig. 11. Effect of different Fe^{2+} dosage and H_2O_2 concentration on cyanide removal (pH of 3, carrier dosage volume of 40%, and aeration flow rate of 0.22 m^3/h).

to the less reactive hydroperoxyl radicals ($HO_2^{\bullet}$) (Eqs. (7) and (8)) [27]. This verifies that the Fe^{2+} and H_2O_2 dosage of 0.24 g/L and 6.0 mL/L was the optimum parameters during this process.

$$H_2O_2 + {}^{\bullet}OH \rightarrow HO_2^{\bullet} + H_2O \quad (7)$$

$$HO_2^{\bullet} + {}^{\bullet}OH \rightarrow H_2O + O_2 \uparrow \quad (8)$$

3.5. Recycling performance and kinetics

The recycling performance of the cyanide and COD removal efficiencies were evaluated during the four recycling of utilization under the above optimal experimental conditions, the experiment result is shown in Fig. 12.

After circulated four times, the YL-2 carrier coated iron oxides still kept high degradation efficiencies of 72% and 74.3% for cyanide and COD, respectively. Compared with the initial 83.6%, cyanide removal efficiency only decreased about 12%, as well as COD. After 5 h of repeated use, the loaded iron content only decreased slightly that from 91.72 to 75.6 mg of mean value each carrier, which indicated that YL-2 carrier coated iron oxides had a certain stability and could be used in the fluidized bed repeatedly.

Further, the rate constants (k) of cyanide removal for the four uses of the catalytic carrier were summarized in Table 6. All cyanide values for the pseudo-second-order reaction rate constant (k) were calculated from the linear regression of the pseudo-second-order kinetic model with related coefficients exceeding 0.93, which was higher than the zero-order and pseudo-first-order model, meant that the reaction could be predicted by this kinetic equation.

3.6. Mechanism discussion

During the fluidized-bed Fenton process, both cyanide and COD showed obvious degradation trend that

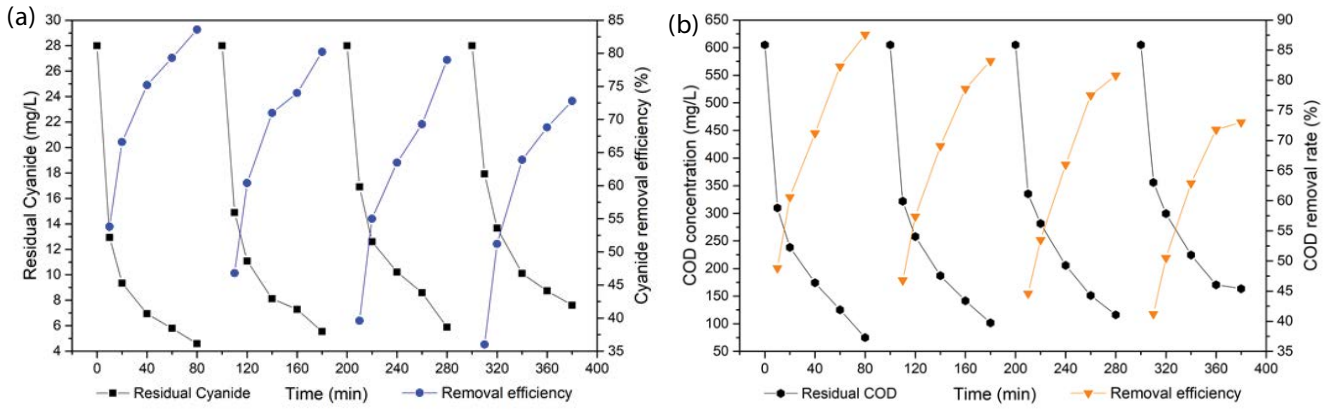

Fig. 12. Evaluation of recycling performance of YL-2 carrier coating iron oxides on cyanide (a) and COD (b) removal (initial pH: 3.0, H_2O_2 initial concentration: 6 mL/L, Fe^{2+} dosage: 0.24 g /L, aeration flow rate: 0.22 m^3/h and carrier dosage volume: 40%).

Table 6
Cyanide degradation kinetic model and parameters

Number of carrier usage	Zero-order kinetic model		Pseudo-first-order kinetic model		Pseudo-second-order kinetic model	
	Rate constant (L mg^{-1} min^{-1})	R^2	Rate constant (L mg^{-1} min^{-1})	R^2	Rate constant (L mg^{-1} min^{-1})	R^2
1	0.1081	0.8360	0.0130	0.9413	0.0019	0.9884
2	0.1205	0.8407	0.0131	0.9331	0.0011	0.9695
3	0.1404	0.8991	0.0136	0.9581	0.0014	0.9316
4	0.1360	0.8210	0.0116	0.9108	0.0012	0.9715

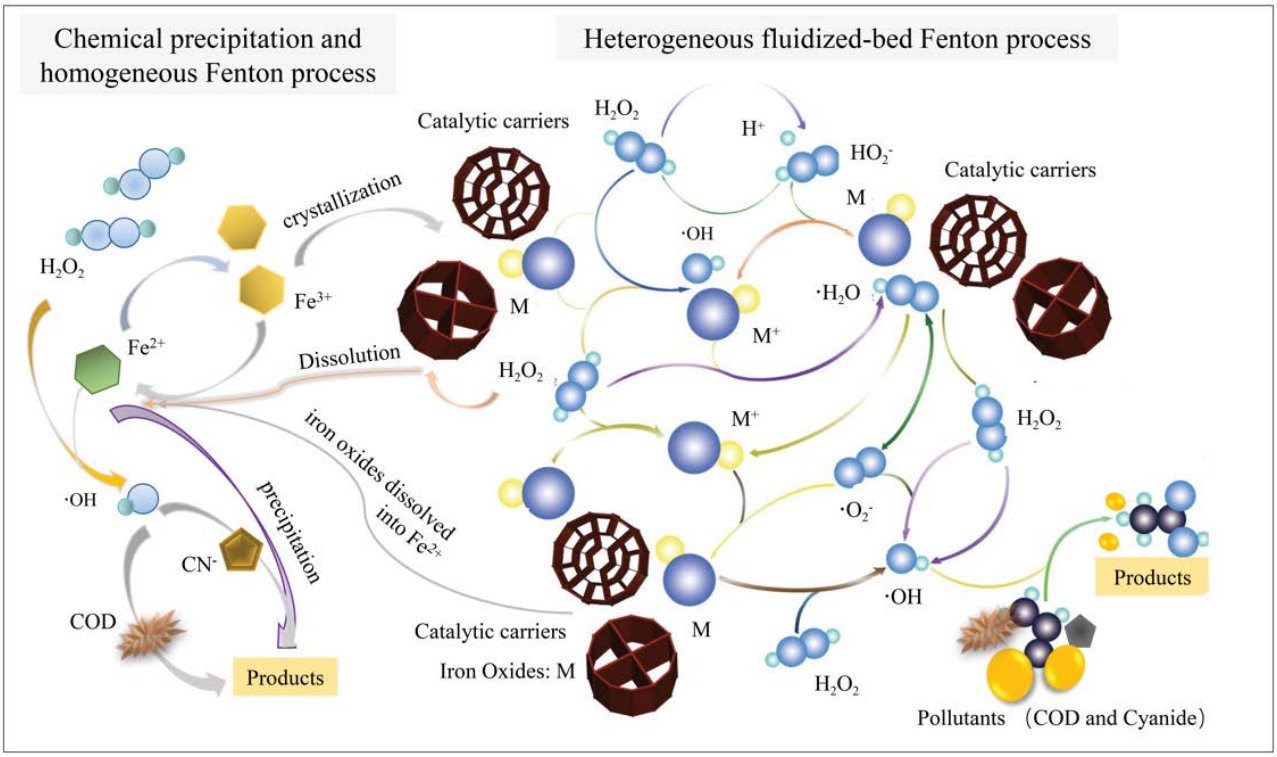

Fig. 13. Schematic diagram of reaction mechanism.

attributed to complex reaction mechanisms include: (a) chemical precipitation (Fe^{2+}/CN^-); (b) homogeneous Fenton (H_2O_2/Fe^{2+}), (c) fluidized-bed crystallization, and (d) reductive dissolution of iron oxides. Experimental results in this paper have proved that the cyanide elimination by chemical precipitation, homogeneous Fenton, and fluidized-bed Fenton process is rising gradually. However, the constant and stable COD degradation indicated that the reaction was dominated by oxidation (•OH) that occurred both in fluidized-bed and homogeneous Fenton process. Cyanide degradation in Fenton fluidized bed system is a complex process, which can be divided into the following steps [21,27,28]:

- homogeneous •OH production from Fe^{2+} and H_2O_2;
- conversion of Fe^{2+} to Fe^{3+}, and slower conversion of Fe^{3+} back to Fe^{2+};
- reaction of CN^-, COD, and •OH.

Additional reactions in fluidized-bed Fenton process are heterogeneous reactions, brought about by the presence of YL-2 suspended carrier are as follows:

- Fe^{3+} crystallization in iron oxide forms initiated by the carrier;
- production of •OH from H_2O_2 catalyzed via iron oxides;
- iron oxides dissolved into Fe^{2+} again.

The mechanism of the above process is shown in Fig. 13. The multiple reaction processes of cyanide and COD removal include direct chemical precipitation, Fenton oxidation and fluidized bed crystallization. The H_2O_2 mainly decomposes into HO_2^- and H^+ ions initially, then the iron oxide (expressed in M in the figure) attached on the surface of the carrier reacts with H_2O_2 to generate M^+ ions and hydroxyl radicals (•OH) further generating H_2O and $•HO_2$ under the function of H_2O_2. Lastly, the H_2O_2 can be reacted with $•O_2^-$ and $•HO_2$,

respectively, to produce large amounts of •OH ions for degrading cyanide and organic pollutants effectively.

4. Conclusions

In this study, the polypropylene light materials coating iron oxide as suspended carrier was successfully prepared and characterized to carry out in the fluidized-bed Fenton process for the treatment of cyanide-containing wastewaters. Compared with the chemical precipitation process, the homogeneous Fenton process under the optimal operating parameters, batch experimental results suggested that the assembled fluidized Fenton system exhibited a higher performance on cyanide and COD degradation, which consumes less Fe^{2+} ions and has higher removal efficiencies and sustainability. The optimum parameters of the experiment are the initial solution pH of 3, Fe^{2+} dosage of 0.24 g/L, H_2O_2 concentration of 6.0 mL/L, aeration flow rate of 0.22 m^3/h, and carrier dosage volume of 40%. After 80 min of reaction, the removal efficiencies of cyanide and COD reached 83.6% and 87.8%, respectively. The oxidized durability of polypropylene light materials coating iron oxide indicated considerable stability for long-term removal of cyanide-containing wastewater. This means that the technique can be employed as a cost-effective method for the degradation of pollutants, without the end-of-pipe discharge of iron sludge into the environment.

Acknowledgments

The authors gratefully acknowledge the financial support from the Major Science and Technology Program for Water Pollution Control and Treatment (No. 2017ZX07402001); the Research Fund of Key research program of Ministry of science and technology for Water resources efficient development and utilization project (No. 2018YFC0406403).

Conflicts of interest

The authors declare no competing financial interest.

References

[1] J. Wei, Y.H. Song, X. Tu, L. Zhao, E.R. Zhi, Pretreatment of dry-spun acrylic fiber manufacturing wastewater by Fenton process: optimization, kinetics and mechanisms, Chem. Eng. J., 218 (2013) 319–326.
[2] C.Y. Zhang, J.L. Wang, H.F. Zhou, D.G. Fu, Z.Z. Gu, Anodic treatment of acrylic fiber manufacturing wastewater with boron-doped diamond electrode: a statistical approach, Chem. Eng. J., 161 (2010) 93–98.
[3] Y. Sun, Y.X. Shen, P. Liang, J. Zhou, Y. Yang, X. Huang, Linkages between microbial functional potential and wastewater constituents in large-scale membrane bioreactors for municipal wastewater treatment, Water Res., 56 (2014) 162–171.
[4] G. Moussavi, R. Khosravi, G. Moussavi, R. Khosravi, Removal of cyanide from wastewater by adsorption onto pistachio hull wastes: parametric experiments, kinetics and equilibrium analysis, J. Hazard. Mater., 183 (2010) 724–730.
[5] P.J.M. Marques, P.M. Reis, C.M. Rui, L.M. Gando-Ferreira, R.M. Quinta-Ferreira, Iron recovery from the Fenton's treatment of winery effluent using an ion-exchange resin, J. Mol. Liq., 242 (2017) 505–511.
[6] L. Wang, Faculty of urban construction and environmental engineering of Chongqing University, Chongqing, 2010.
[7] M.Q. Qiu, C. Huang, A comparative study of degradation of the azo dye C.I. acid blue 9 by Fenton and Photo-Fenton oxidation, Desal. Wat. Treat., 24 (2010) 273–277.
[8] A.J. Expósito, J.M. Monteagudo, N.A. Durã, M.I. San, L.L. Gonzã, Study of the intensification of solar photo-Fenton degradation of carbamazepine with ferrioxalate complexes and ultrasound, J. Hazard. Mater., 21 (2017) 156–184.
[9] Y. Du, M. Zhou, L. Lei, Y. Du, M. Zhou, L. Lei, Kinetic model of 4-CP degradation by Fenton/O_2 system, Water Res., 41 (2007) 1121–1133.
[10] E. Mousset, S. Pontvianne, M.N. Pons, Fate of inorganic nitrogen species under homogeneous Fenton combined with electro-oxidation/reduction treatments in synthetic solutions and reclaimed municipal wastewater, Chemosphere, 201 (2018) 6–12
[11] A.N. Soon, B.H. Hameed, Heterogeneous catalytic treatment of synthetic dyes in aqueous media using Fenton and photo-assisted Fenton process, Desalination, 269 (2011) 1–16.
[12] J. Li, Z. He, Optimizing the performance of a membrane bio-electrochemical reactor using an anion exchange membrane for wastewater treatment, Environ. Sci. Water Res. Technol., 1 (2015) 355–362.
[13] J. Anotai, C.M. Chen, L.M. Bellotindos, M.C. Lu, Treatment of TFT-LCD wastewater containing ethanolamine by fluidized-bed Fenton technology, Bioresour. Technol, 113 (2012) 272–275.
[14] N. Boonrattanakij, M.C. Lu, J. Anotai, Iron crystallization in a fluidized-bed Fenton process, Water Res., 45 (2011) 3255–3262.
[15] A. Mirzaei, Z. Chen, F. Haghighat, L. Yerushalmi, Removal of pharmaceuticals from water by homo/heterogonous Fenton-type processes-a review, Chemosphere, 174 (2017) 665–688.
[16] N. Masomoon, C. Raranatamskul, M.C. Lu, Chemical oxidation of 2,4 - dimethylaniline in the Fenton process, Environ. Sci. Technol., 43 (2009) 8629–8634.
[17] J. Liu, J. Li, R.W. Mei, F.C. Wang, B. Sellamuthu, Treatment of recalcitrant organic silicone wastewater by fluidized-bed Fenton process, Sep. Purif. Technol., 132 (2014) 16–22.
[18] J.A. Donadelli, L. Carlos, A. Arques, F.S.G. Einschlag, Kinetic and mechanistic analysis of azo dyes decolorization by ZVI-assisted Fenton systems: pH-dependent shift in the contributions of reductive and oxidative transformation pathways, Appl. Catal., B., 5 (2018) 51–61.
[19] D.L. Xi, Y.S. Sun, X.Y. Liu, Environmental Monitoring, Higher Education Press, Beijing, 2004.
[20] J.W. Tang, K. Ning, W.X. Lei, C.H. Zhang, X.F. Meng, Treatment of acrylic fiber wastewater by Fenton fluidized bed oxidation process with suspended filler coated iron oxide, Chem. Ind. Eng. Pro.(China), 37 (2018) 4476–4479 http://kjs.mee.gov.cn/hjbhbz/.
[21] J.L. Yan, X.J. Wang, Y.X. Li, Study on dying wastewater treatment by Fenton-fluidized bed process with iron oxide coated sand, Technol. Water Treat. (China), 38 (2012) 76–78.
[22] Y. Lee, U.V. Gunten, Advances in predicting organic contaminant abatement during ozonation of municipal wastewater effluent: reaction kinetics, transformation products, and changes of biological effects, Environ. Sci. Water Res. Technol., 2 (2016) 421–442.
[23] E.M. Matira, T.C. Chen, M.C. Lu, M.L.P. Dalida, Degradation of dimethyl sulfoxide through fluidized-bed Fenton process, J. Hazard. Mater., 13 (2016) 1017–1028.
[24] H.Y. Li, R. Priambodo, Y. Wang, H. Zhang, Y.H. Huang, Mineralization of bisphenol A by Photo-Fenton-like process using a waste iron oxide catalyst in a three-phase fluidized bed reactor, J. Taiwan Inst. Chem. Eng., 53 (2015) 68–73.
[25] N.H.M. Azmi, O.B. Ayodele, V.M. Vadivelu, M. Asif, B.H. Hameed, Fe-modified local clay as effective and reusable heterogeneous Photo-Fenton catalyst for the decolorization of Acid Green 25, J. Taiwan Inst. Chem. Eng., 45 (2014) 1459–1467.
[26] C.C. Su, P.A. Massakul, R. Chavalit, M.C. Lu, Effect of operating parameter on decolorization and COD removal of three reactive dyes by Fenton's reagent using fluidized-bed reactor, Desalination, 278 (2011) 211–218.
[27] D. Huang, C. Hu, G. Zeng, M. Cheng, P. Xu, X. Gong, Combination of Fenton processes and biotreatment for wastewater treatment and soil remediation, Sci. Total Environ., 574 (2017) 1599–1610.
[28] J. Xu, Y. Long, D. Shen, H. Feng, T. Chen, Optimization of Fenton treatment process for degradation of refractory organics in pre-coagulated leachate membrane concentrates, J. Hazard. Mater, 323 B (2017) 674–680.